Bufalin suppresses esophageal squamous cell carcinoma progression by activating the PIAS3/STAT3 signaling pathway

Qianqian Ju[1]^, Qinyan Shi[2], Cheng Liu[2], Guolong Fu[2], Hui Shi[3]^

[1]Medical College of Nantong University, Nantong, China; [2]Zhongke Gene Biotechnology, Nantong, China; [3]Department of Thoracic Surgery, Shanghai Chest Hospital, School of Medicine, Shanghai Jiao Tong University, Shanghai, China
Contributions: (I) Conception and design: Q Ju, H Shi; (II) Administrative support: Q Shi; (III) Provision of study materials or patients: Q Ju, Q Shi, C Liu, G Fu; (IV) Collection and assembly of data: Q Ju, Q Shi, C Liu, G Fu; (V) Data analysis and interpretation: Q Ju, H Shi; (VI) Manuscript writing: All authors; (VII) Final approval of manuscript: All authors.
Correspondence to: Hui Shi, MD. Department of Thoracic Surgery, Shanghai Chest Hospital, School of Medicine, Shanghai Jiao Tong University, 241 Huaihaixi Road, Shanghai 200030, China. Email: disney1982@163.com.

Background: Esophageal cancer, especially esophageal squamous cell carcinoma (ESCC), is a common malignant tumor of the digestive tract. Bufalin is an effective anti-tumor compound. However, little is known about the regulatory mechanisms of Bufalin in ESCC. To investigate the effect and molecular mechanism of Bufalin on the proliferation, migration and invasion of ESCC cells will provide a more reliable basis for the application of Bufalin in clinical tumor therapy.

Methods: First, the half-inhibitory concentration (IC50) of Bufalin was evaluated by Cell Counting Kit-8 (CCK-8) assays. *In vitro*, the effects of Bufalin on the proliferation of the ECA109 cells was measured using CCK-8 and 5-ethynyl-2'-deoxyuridine assays. Wound-healing and transwell assays were used to evaluate the effects of Bufalin on the migration and invasion of the ECA109 cells. Further, to determine the mechanisms underlying the Bufalin-mediated suppression of cell progression in ESCC, total RNA was extracted from negative control (NC) and Bufalin treated cells to perform RNA-sequencing (RNA-seq) to screen for abnormally expressed genes. *In vivo*, the ECA 109 cells were subcutaneously injected into BALB/c nude mice to determine the effects of Bufalin on tumor cell proliferation. The protein inhibitor of activated signal transducer and activator of transcription 3 (PIAS3), signal transducer and activator of transcription 3 (STAT3), and phosphorylated STAT3 (p-STAT3) protein expression levels in the ECA109 cells were detected by Western blot.

Results: The CCK-8 assays showed that the IC50 of Bufalin was 200 nM. The proliferation, migration, and invasion ability of the ECA109 cells was significantly inhibited in the Bufalin group in a concentration-dependent manner. *In vivo*, the Xenograft tumor model showed that Bufalin decreased the tumor volume and weight of the subcutaneous tumors. The RNA-seq results showed that the expression of PIAS3 was upregulated in the Bufalin group. Additionally, down-regulation of PIAS3 decreased the inhibition of STAT3, thereby increasing p-STAT3 expression. Finally, PIAS3 knockdown reversed the inhibitory effects of Bufalin on the proliferation, migration, and invasion of the ECA109 cells.

Conclusions: Bufalin may inhibit the proliferation, migration, and invasion of the ECA109 cells through the PIAS3/STAT3 signaling pathway.

Keywords: Esophageal squamous cell carcinoma (ESCC); protein inhibitor of activated signal transducer and activator of transcription 3 (PIAS3); proliferation; migration; invasion

---

^ ORCID: Qianqian Ju, 0000-0001-7561-1058; Hui Shi, 0000-0001-6446-4160.

Introduction

Esophageal cancer (EC) is one of the most common malignant tumors of the upper digestive tract in the world (1). Recently, the International Agency for Research on Cancer of the World Health Organization reported that in 2020, there were 600,000 new cases of EC and 540,000 EC-related deaths worldwide, making it the 8th most common cancer, and the 6th leading cause of cancer-related deaths (2,3). EC is also one of the top 10 malignant tumors in China, and with 320,000 new cases and 300,000 deaths, it was the 6th most common cancer and the 4th leading cause of cancer-related deaths in 2020 in China (4). The two main histological types of EC are esophageal squamous cell carcinoma (ESCC) and esophageal adenocarcinoma (5). Among them, ESCC is the main histological type of EC in China (6). EC has strong invasiveness and high mortality. Due to the lack of early and specific clinical symptoms, most EC patients are only diagnosed in the late stage.

In recent years, a small number of EC patients have benefited from the development of diagnostic technology, the optimization of radiotherapy and chemotherapy, and the improvement of surgical procedures (7). However, a considerable number of EC patients still develop metastasis and recurrence after surgery. The 5-year survival rate of EC patients after surgery is <20% (8). EC seriously endangers the health of people all over the world. EC has a poor

prognosis because it is prone to local invasion and distant lymph node metastasis. To develop more effective diagnosis and treatment methods and molecular-targeted therapies for EC, the molecular pathological mechanism underlying the occurrence, development, and metastasis of EC urgently needs to be explored and studied.

In recent years, traditional Chinese medicine (TCM) has been shown to have good clinical effects in the treatment of tumors, which can significantly improve the survival time of patients (9-11). Bufalin is a major anti-tumor component extracted from the TCM Venenum Bufonis (12). Bufalin belongs to cardiotonic glycosides and has a wide range of pharmacological effects. Previous studies have shown that Bufalin kills a variety of solid tumors and hematological tumors, such as prostate tumor (13,14), liver tumor (15,16), gastric tumor (17,18), ovarian tumor (19), and leukemia (20). The mechanism involves the following aspects: the inhibition of cell proliferation, the induction of differentiation, the induction of apoptosis, the destruction of the cell cycle, the inhibition of tumor angiogenesis, the reversal of multidrug resistance, and the regulation of the immune response. In addition to its anti-tumor effects, Bufalin can also act as an active agent to enhance the sensitivity of tumors to chemotherapeutic drugs, and even reverse drug resistance in some tumors, such as liver cancer (21,22). Thus, the TCM Bufalin may be able to be used in the clinical treatment of tumors in the future. Studies have found that Bufalin is a broad-spectrum anti-tumor drug (23). At present, it has shown its anti-tumor activity in the clinical treatment of leukemia, liver cancer, gastric cancer and other tumors (24,25). A study has found that Bufalin can inhibit the proliferation of vascular endothelial cells in a variety of tumor tissues, affect its neovascularization, and then inhibit tumor growth (26). In leukemia-related study, it was found that Bufalin could significantly inhibit the growth of leukemic cells and induce their differentiation and apoptosis (25). Studies have shown that Bufalin can activate members of Caspase family and Bcl-2 family, promote the formation of Bax homodimer (27), and activate hydrolases such as Caspase-8, Caspase-9 and Caspase-3, which significantly increase the permeability of mitochondrial membrane and lead to the release of cytochrome C into the cytoplasm. And then induce apoptosis of tumor cells (23). It has been reported that XanduLing can effectively reverse the resistance to retinoic acid during chemotherapy in acute promyelocytic leukemia and restore chemosensitivity (28). Cytological

---

Highlight box

Key findings
- Bufalin suppressed ESCC progression by activating the PIAS3/STAT3 signaling pathway.

What is known and what is new?
- Bufalin is a main antitumor component extracted from the traditional Chinese medicine, Venenum Bufonis. Bufalin kills a variety of solid and hematological tumors.
- The effects of Bufalin on the proliferation, migration, and invasion of ESCC cells has not yet been fully elucidated. We found that Bufalin inhibited the proliferation, migration, and invasion of ECA109 cells. We also revealed that Bufalin may inhibit the proliferation, migration, and invasion of the ECA109 cells and upregulate the expression of PIAS3. Thus, inhibit the activity of STAT3, and downregulate the expression of p-STAT3.

What is the implication, and what should change now?
- Further research on the role and molecular mechanism of Bufalin in ESCC and other malignant tumors will provide a more reliable basis for its application in clinical tumor therapy.

studies showed that Bufalin could inhibit the expression of proliferation-related genes in HL-60 cell line, down-regulate the expression of cyclin and induce cell cycle arrest (29,30), and further induce the activation of cell apoptosis. It is believed that with the development of modern Chinese medicine, the active components of Bufalin can play a more important role in anti-tumor therapy (31). In recent years, scholars in China and abroad have confirmed that Bufalin effectively promotes the apoptosis of EC cells (32), and its possible molecular mechanism has been studied from different aspects. However, the effects of Bufalin on the proliferation, migration, and invasion of ESCC cells has not yet been fully elucidated. In this study, we mainly sought to examine the inhibitory effects of Bufalin on the proliferation, migration, and invasion of ECA109 cells, and explore its potential molecular mechanism.

The protein inhibitor of activating signal transducer and activator of transcription 3 (PIAS3) is a small ubiquitin-like regulatory factor-E3 (SUMO-E3) ligase, which catalyzes the covalent binding of small ubiquitin-like modifier (SUMO) protein to specific target substrates and directly binds to the DNA binding domain of phosphorylated STAT3 (p-STAT3) protein (33), thus specifically inhibiting STAT3 activation. The overactivation of STAT3 may play an important role in the occurrence of a variety of tumors (34). Researchers have also studied the expression level of its inhibitor PIAS3 in tumors. Zhang *et al.* found that the expression of PIAS3 in glioblastoma cell lines was significantly suppressed at the post-transcriptional level (35). However, other studies have found that the expression level of PIAS3 in human lung cancer (36,37), breast cancer (38,39), prostate cancer (40), and colorectal cancer (41) is significantly increased. Thus, PIAS3 may play different roles in different types of tumors. The role of PIAS3 in the occurrence and development of ESCC has not yet been reported.

In this study, ECA109 cells were used as a model to observe the effects of Bufalin on the proliferation, migration, and invasion of ECA109 cells. A transplanted tumor model of nude mice was used to evaluate the effects of Bufalin on the progression of EC. This study sought to clarify the biological role of Bufalin in the occurrence and development of EC and to explore its potential mechanism, and thus provide an experimental basis for the clinical application of Bufalin in the treatment of EC. We present the following article in accordance with the MDAR and ARRIVE reporting checklists (available at https://jtd.amegroups.com/article/view/10.21037/jtd-23-486/rc).

Methods

Patient tissues

In 2015, samples from 20 patients who had been pathologically diagnosed with invasive ESCC were collected from the Department of Pathology of Shanghai Tenth People's Hospital. At the same time, the corresponding adjacent normal tissues (pathologically confirmed well-differentiated squamous epithelium >2 cm from the cancer) were collected to serve as the control. The patients' ages ranged from 45 to 80 years, and 12 were male and 8 were female. None of the patients had a history of other tumors or autoimmune diseases, and none had received radiotherapy, chemotherapy or immunosuppressive therapy before the surgery. The EC and paracancerous tissues were put into cryopreservation tubes and immediately cryopreserved in liquid nitrogen for the subsequent tissue RNA extraction. ESCC was confirmed in all the tissue specimens by the chief pathologist. This experiment was done in Shanghai Tenth People's Hospital. The collection of all the ESCC specimens was approved by the Ethics Committee of Shanghai Tenth People's Hospital (No. SHSY-IEC-4.1/21-78/02), and the informed consent of patients was obtained. The study was conducted in accordance with the Declaration of Helsinki (as revised in 2013).

Antibodies and reagents

Bufalin was purchased from Sigma (Cat# B0261) (St. Louis, MO, USA). Antibodies to PIAS3 (Cat# 9042, RRID: AB_2797692), STAT3 (Cat# 12640, RRID: AB_2629499), p-STAT3 (Cat# 9145, RRID: AB_2491009), and β-actin (Cat# 3700, RRID: AB_2242334) were purchased from Cell Signaling Technology (Danvers, MA, USA). The horseradish peroxidase (HRP)-conjugated goat anti-rabbit immunoglobulin G (IgG; Cat# AP187P), and HRP-conjugated goat anti-mouse IgG (Cat# AP181P) were purchased from Sigma (St. Louis, MO, USA).

Immunohistochemistry (IHC)

Paraffin-embedded specimens were successively sliced according to the standard of 4 μM. Baked the slices in 60 ℃ for 4 hours. Then, put them in a slicing box for use. The slides were baked in 65 ℃ for 2 h before dyeing and put in xylene solution I and xylene solution II respectively for dewaxing for 10 min ×2 times. Then the slides were soaked in 100% ethanol I for 10 min, 100% ethanol II

for 10 min and 95% ethanol, 90% ethanol, 80% ethanol and 70% ethanol for 5 min, respectively, for gradient ethanol hydration. The slides were soaked and rinsed in phosphate-buffered saline (PBS) solution for 5 min. After 3 times, citric acid antigen repair solution was added for antigen repair at high-temperature (the slides were heated in a microwave oven for 20 min, and allowed to naturally cool to room temperature). The slides were rinsed in PBS buffer solution for 5 min ×3 times and then wiped the sections. 3% hydrogen peroxide (H_2O_2) was added to block the endogenous peroxidase, and incubated the slides for 10 min (in the dark, at room temperature). Goat serum was dripped onto the slides and blocked for 30 min (37 ℃). The serum was removed from the slides. The slides were placed in the moisturizing box. The first antibody working solution was dripped (the concentration of PIAS3 antibody was 1:200), and kept overnight at 4 ℃. After the slides were soaked and rinsed with PBS buffer solution, the biotin labeled secondary antibody working solution was dropped on the slides and incubated in a wet box for 1 h (37 ℃). Then the slides were dropped the working solution of streptavidin labeled with HRP and incubated for 1 h (37 ℃). Next, both 3,3N-diaminobenzidine tetrahydrochloride (DAB) color development and hematoxylin counterstaining were performed. Finally, gradient ethanol dehydration was performed, the xylene was made transparent, the neutral gum was dropped, and the glass was covered. Brown or light-yellow granules indicated the positive expression of PIAS3, and PIAS3 was mainly located in the nucleus. Based on the dyeing degree, the final dyeing result were scored as follows: 0 = colorless, 1 = light yellow, 2 = brown-yellow, and 3 = brown. According to the percentage of positive cells, the percentages of 1–10%, 11–50%, 51–75%, and >75%, were scored as 1, 2, 3, and 4, respectively. The total score was obtained by multiplying the two scores above. The results were characterized as follows: 9–12 points, strong positive staining (3+); 6–8 points, moderate positive staining (2+); 4–5 points, weak positive staining (1+); and 0–3 points, negative staining (–). Moderate positive and strong positive staining indicated a high expression of PIAS3, while weak positive and negative are staining indicated a low expression.

Cell culture and siRNA transfection

Human ESCC cell line ECA109 (CC-Y1150) was purchased from Shanghai Cell Bank (Shanghai Biological Sciences, Chinese Academy of Sciences, Shanghai, China).

The ECA109 cells were adherent cells and were cultured in Petri dishes. After successful resuscitation, the ECA109 cells were added to a complete culture medium composed of Dulbecco's modified Eagle's medium (DMEM; Gibco, Carlsbad, CA) containing 100 U/mL of penicillin and 100 μg/mL of streptomycin (Solarbio, Beijing, China) and fetal bovine serum (FBS) (Lonsera, Shanghai, China) at a ratio of 9:1, and put into a 5% carbon dioxide (CO_2), 37 ℃ incubator for routine culture, and the solution was changed the next day.

The small-interfering RNAs (siRNAs) targeting human PIAS3 were purchased from Genepharma (Shanghai, China) with the following sequences: PIAS3 siRNA-1#, 5'-GCAGGAACCCTTCTACAAA-3'; PIAS3 siRNA-2#, 5'-GGAGATCCATCAGAGAATA-3'; PIAS3 siRNA-3#, 5'-GTGATGAGATCCAATTCAT-3'. The ECA109 cells were transfected with 80 nM of siRNA using Lipofectamine 8000 (Invitrogen, CA, USA) for 48 h.

RNA isolation and quantitative real-time polymerase chain reaction (qRT-PCR)

The cells or tissues from which the RNA was to be extracted, and rinsed twice with PBS solution, after which TRIzol LS Reagent (Invitrogen, Carlsbad, CA) was added to extract the total RNA. Next, 30 μL of RNase-free diethyl pyrocarbonate (DEPC) water was added to the RNA precipitated tube, and the tube was left to stand at room temperature for 2 min to dissolve the RNA. The RNA concentration and purity were detected using the Nano Drop system (Thermo Scientific). For each group, 1 μg of RNA underwent reverse transcription according to the instructions of the reverse transcription kit (Takara). The reaction conditions were as follows: 50 ℃ for 15 min, and 85 ℃ for 5 s. The complementary DNA solution was stored in a refrigerator at –20 ℃ awaiting use. qRT-PCR was performed using SYBR Green Master mix (Roche Diagnostics, Basel, Switzerland) on a Lightcycler 96 system (Roche, Basel, Switzerland). The reaction procedure was as follows: pre-denaturation at 95 ℃ for 5 min, denaturation at 95 ℃ for 10 s, annealing at 60 ℃ for 30 s, and extension at 65 ℃ for 30 s for 40 cycles. The results were analyzed by $2^{-\Delta\Delta Ct}$. All the primers were designed and synthesized by Shanghai Sangon Biological Company, and glyceraldehyde-3-phosphate dehydrogenase (GAPDH) was used as the internal reference gene. The specific primer sequences were as follows: PIAS3-F CGGACGGAATTACTCCTTGTCTGTG,

PIAS3-R GTCAGGGTCAGCAGTCAATTTCTCC; GAPDH-F GACCTGACCTGCCGTCTA, GAPDH-R AGGAGTGGGTGTCGCTGT.

Western blot analysis

Human ECA109 cells in the logarithmic growth phase in good condition were cultured in 6-well plates, the culture medium was removed, the cells were washed 3 times with PBS, and the residual liquid was removed. Next, 200 µL of protein lysate [containing protease inhibitor and phenylmethylsulfonyl fluoride (PMSF) premix] was added to each well, and the cells were then scraped and moved into a precooled 1.5-mL Eppendorf (EP) tube. The cells were cracked on ice for 10–15 min, and then centrifuged at 4 ℃, 1,2000 rpm for 30 min. After that, took the supernatant, and moved it into a precooled EP tube. Protein concentration was determined using the BCA method in accordance with the instructions of the BCA protein sample determination kit (Thermo Scientific). The absorbance [optical density (OD)] value at the wavelength of 570 nm was measured on a microplate reader (Thermo Scientific), the standard curve was drawn using the OD value of the standard sample, and the total protein concentration of the protein sample was calculated. Next, 5× loading buffer was added to the tube. The tube was denatured at 100 ℃ for 5 min. Then, 10% sodium dodecyl-sulfate polyacrylamide gel electrophoresis gel was prepared, and the denatured protein was carefully added to each well for electrophoresis, and the protein was then transferred to the 0.45-µm polyvinylidene fluoride (PVDF) membrane. After the end of transmembrane the PVDF membrane was taken out and placed in the blocking buffer (containing 5% skim milk powder). After incubation at room temperature for 1 h, the membrane was taken out of the blocking buffer and washed 3 times with Tris-Buffered Saline with Tween (TBST; Tween 20:Tris-Buffered Saline =1:1,000) for 5 min each time. The membrane was incubated with primary antibody PIAS3, p-STAT3, STAT3, and β-actin, and kept overnight at 4 ℃. After the TBST membrane had been washed for 10 min for 3 times each, diluted HRP-labeled secondary antibody (1:10,000) was added, and the membrane was incubated in a transference decoloring shaker at room temperature for 1 h. Finally, taking β-actin as an internal reference. Enhanced chemiluminescence (ECL) detection was performed using a chemiluminescence instrument and protein bands were collected. ImageJ software (National Institutes of Health) was used to quantified the bands. The relative expression of the target protein was calculated as follows: relative expression = gray value of target protein/gray value of β-actin.

Cell Counting Kit-8 (CCK-8) assays

The half-inhibitory concentration (IC50) of Bufalin in the ECA109 cells and the effects of Bufalin on the proliferation of the ECA109 cells were detected using the CCK-8 method. The cells in the logarithmic growth phase were digested and made into a single cell suspension, and the cells were then inoculated in 96-well plates, with about 1×10^3 cells inoculated in each well; each group had 3 duplicate wells. The cells were cultured at 37 ℃ in a cell incubator containing 5% CO_2 for 24 and 48 h, respectively. Next, 10 µL of CCK-8 solution (Dojindo Molecula Technologies) was added to each well, and then the cells were continued to incubate in cell incubator in the dark for 4 h. Finally, the OD value at 450 nm was detected by using a Microplate Reader (BioTek Instruments). Light was avoided during the procedure. To determine the IC50 of Bufalin in the ECA109 cells, after the cells were inoculated in 96-well plates, 8 dose groups of 0, 10, 100, 200, 400, 600, 800, and 1,000 nM were set, and each dose group had 3 repeat wells. After 24 h of culturing, cell survival was detected using the CCK-8 method.

Transwell assays

For the transwell migration assays, each group of the ECA109 cells were first digested with 0.25% ethylene diamine tetraacetic acid (EDTA) trypsin solution, and then suspended by adding the complete culture medium. The cells were suspended in DMEM and counted, and the cell concentration was adjusted to 5×10^5 cells /mL. DMEM containing 10% FBS was added to the lower chamber of the transwell chamber, and the prepared cell suspension of each group was added to the upper chamber. Independent experiments were performed at least three times. The cells were incubated in an incubator at 37 ℃ and 5% CO_2 for 24 h. Next, the culture medium was discarded and the cells were washed twice with PBS. The cells were successively fixed with 4% paraformaldehyde (PFA) at room temperature for 30 min, and stained with 0.1% crystal violet (Beyotime Institute of Biotechnology) for 30 min. Then wiped the cells in the upper chamber with a cotton swab. The number of migrating and invading cells was observed, counted and photographed under an inverted microscope. For the transwell invasion experiment, the upper chambers were

coated with Matrigel matrix (50 µL/well, BD Biosciences) before seeding the cells. The other procedures are the same as those of the transwell migration experiment.

Wound-healing assays

Horizontal lines (≥3 lines/holes) were marked with a marker pen at the bottom of the 6-well plate. The ECA109 cells of each group were digested with trypsin and re-suspended in the complete culture medium. The adjusted concentration of the cell suspension (3×10^5 cells/mL) was inoculated into a 6-well plate (200 µL/well) and incubated in a cell incubator until the monolayer cells were formed. Scratch wounds were manipulated with the tip of a 100 µL pipette to scrub the cells (the scratch was perpendicular to the horizontal line at the bottom of the plate) using when the cell density reached above 90%. Washed cells twice with PBS. DMEM medium was added to the cells to continue culture for 24 and 48 h. The migration of the cells at different time points was observed under an inverted microscope (Leica DM IL LED) and photographed. The average scratch width of the cells in each group was measured and calculated by ImageJ software (National Institutes of Health), and the relative migration distance of the cells was calculated.

RNA-sequencing (RNA-seq)

Total RNA from the NC and Bufalin group was extracted using TRIzol (Takara) in accordance with the manufacturer's procedure. The messenger RNA-sequencing (mRNA-seq) was conducted by Sino-science Gene Technology (Shanghai, China). The RNA-seq data presented in this study have been deposited in the Gene Expression Omnibus (GEO) database.

Animal model

The tumorigenic potency of the ECA109 cells was examined using 5-week-old, male BALB/c nude mice (line Source: Beijing Vitong Lihua, Cat# 401) that were obtained from the Animal Center of the Chinese Academy of Science (Shanghai, China). The online tool Quickcalcs (GraphPad Software) was used to randomize the animals for the group assignments. The mice were randomly and blindly assigned to 2 groups (i.e., the negative control (NC) group and the Bufalin group) (n=5 mice per group, total n=10 mice) and maintained under pathogen-free conditions. Cells (2×10^6 cells/200 µL PBS) were injected subcutaneously into the

nude mice. The NC group was intraperitoneally injected with corn oil, while the Bufalin group was intraperitoneally injected with 0.2 mg/kg of Bufalin every day. The nude mice were monitored at an interval of 3 days for the appearance of tumors. The mice were sacrificed by CO_2 asphyxiation on the 25th day after injection, and tumor size and weight were measured. Tumor size was calculated using the following equation: tumor size $= 1/2$ length $\times$ width^2. The whole experiment was conducted by 2 uninformed researchers. Animal experiments were performed under a project license (No. S20200323-186) granted by Institutional Animal Care and Use Committees of the Nantong University, in compliance with the institutional guidelines for the care and use of animals. A protocol was prepared before the study without registration.

Statistical analysis

All the experiments were replicated 3 times in the laboratory. All the data were analyzed using GraphPad Prism 8.0 (GraphPad Software, San Diego, CA, USA). All the data are expressed as the mean ± standard error mean. One-way analysis of variance was used to analyze the data, and Tukey's post hoc test was used to analyze the differences between specific groups. P value <0.05 indicated a statistically significant difference.

Results

Bufalin inhibits the proliferation, migration, and invasion of ECA109 cells

First, to determine the IC50 of Bufalin on the ECA109 cells, we treated the ECA109 cells with 0, 10, 100, 200, 400, 600, 800, and 1,000 nM of Bufalin. The CCK-8 results showed that after 24 h of Bufalin treatment, the inhibition effect on the ECA109 cells increased as the Bufalin concentration increased, and the increase was statistically significant compared to that of the NC group (P<0.001) (*Figure 1A*). When the Bufalin concentration was 200 nM, the cell viability decreased by 46.18%, so we took 200 nM as the IC50. Next, we treated the ECA109 cells with 200 nM of Bufalin for 24 h and tested the effects of Bufalin on the proliferation of the ECA109 cells through CCK-8 and 5-ethynyl-2'-deoxyuridine (EdU) experiments. The results showed that Bufalin significantly reduced the proliferation of the ECA109 cells (*Figure 1B-1D*). Similarly, we also found that the weight and volume of the subcutaneous tumors in
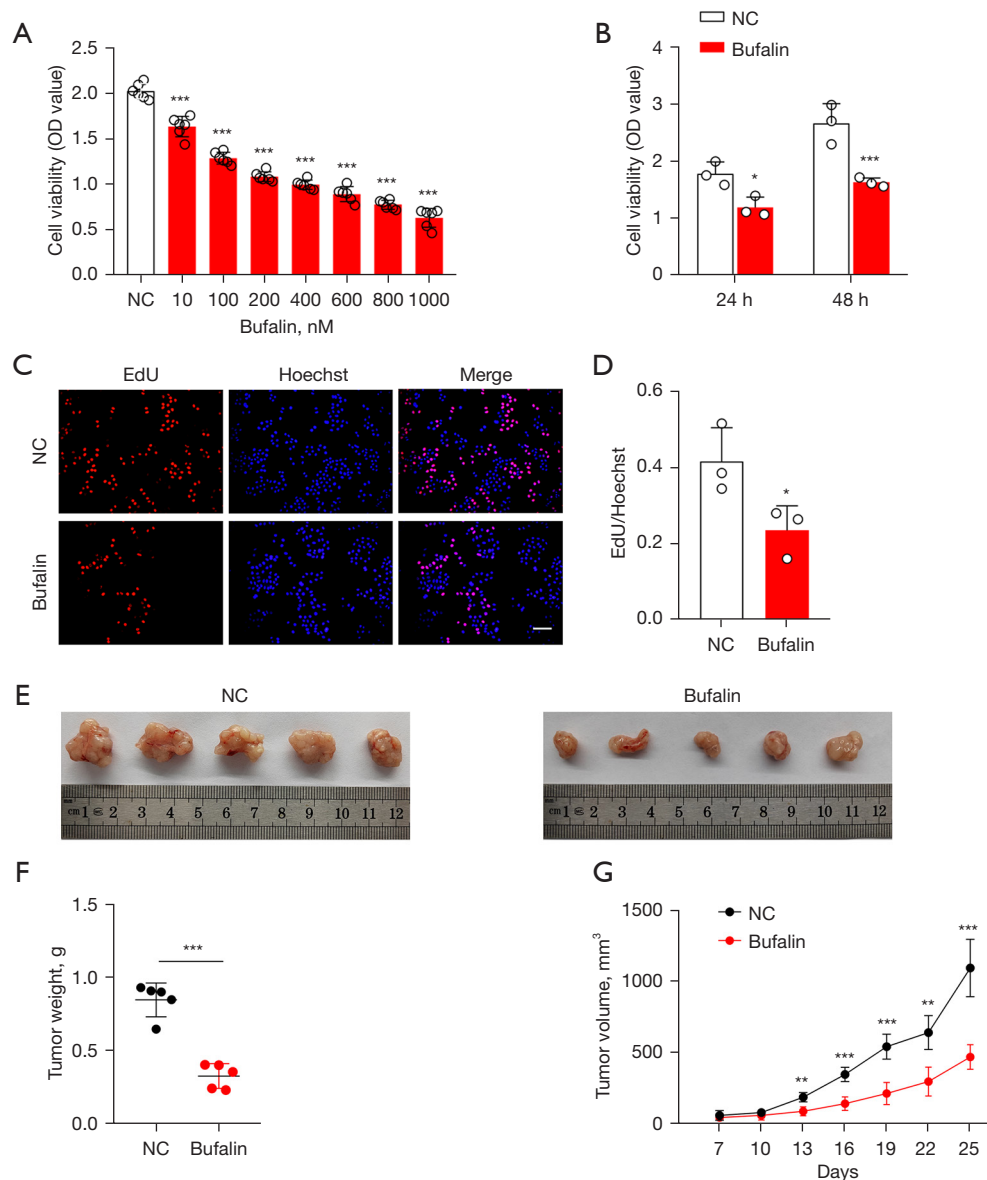
Figure 1 Bufalin inhibits proliferation of ECA109 cells. The viability of ECA109 cells treated with different concentrations of Bufalin for 24 h. The viability of ECA109 cells treated with different concentrations of Bufalin for 24 h (A) and 200 nM Bufalin for different time periods (B) was analyzed by CCK-8 assay. (C) The effect of Bufalin on cell proliferation was measured by EdU assay (scale bar =500 μm). (D) The statistics result of EdU assay. (E) Xenograft model in nude mice; representative images of tumors from all mice in each group (n=5). Mean tumor weights (F) and tumor volume growth curves (G) for tumors formed by the ECA109 cells. X axis represents the number of days after subcutaneous inoculation of ECA109 cells. Data are presented as mean ± SD (error bars). Statistical significance was tested by unpaired Student's t-test. *, $P<0.05$; **, $P<0.01$; ***, $P<0.001$. CCK-8, Cell Counting Kit-8; EdU, 5-ethynyl-2'-deoxyuridine; NC, negative control; OD, optical density; SD, standard deviation.

the nude mice injected intraperitoneally with Bufalin were significantly smaller than those of the mice in the NC group ($P<0.001$) (*Figure 1E-1G*). The above *in vitro* and *in vivo* results showed that Bufalin significantly inhibited the proliferation of the ECA109 cells. In addition, to examine the effects of Bufalin on the migration and invasion of the ECA109 cells, we conducted wound-healing and transwell assays, and found that the number of transmembrane cells
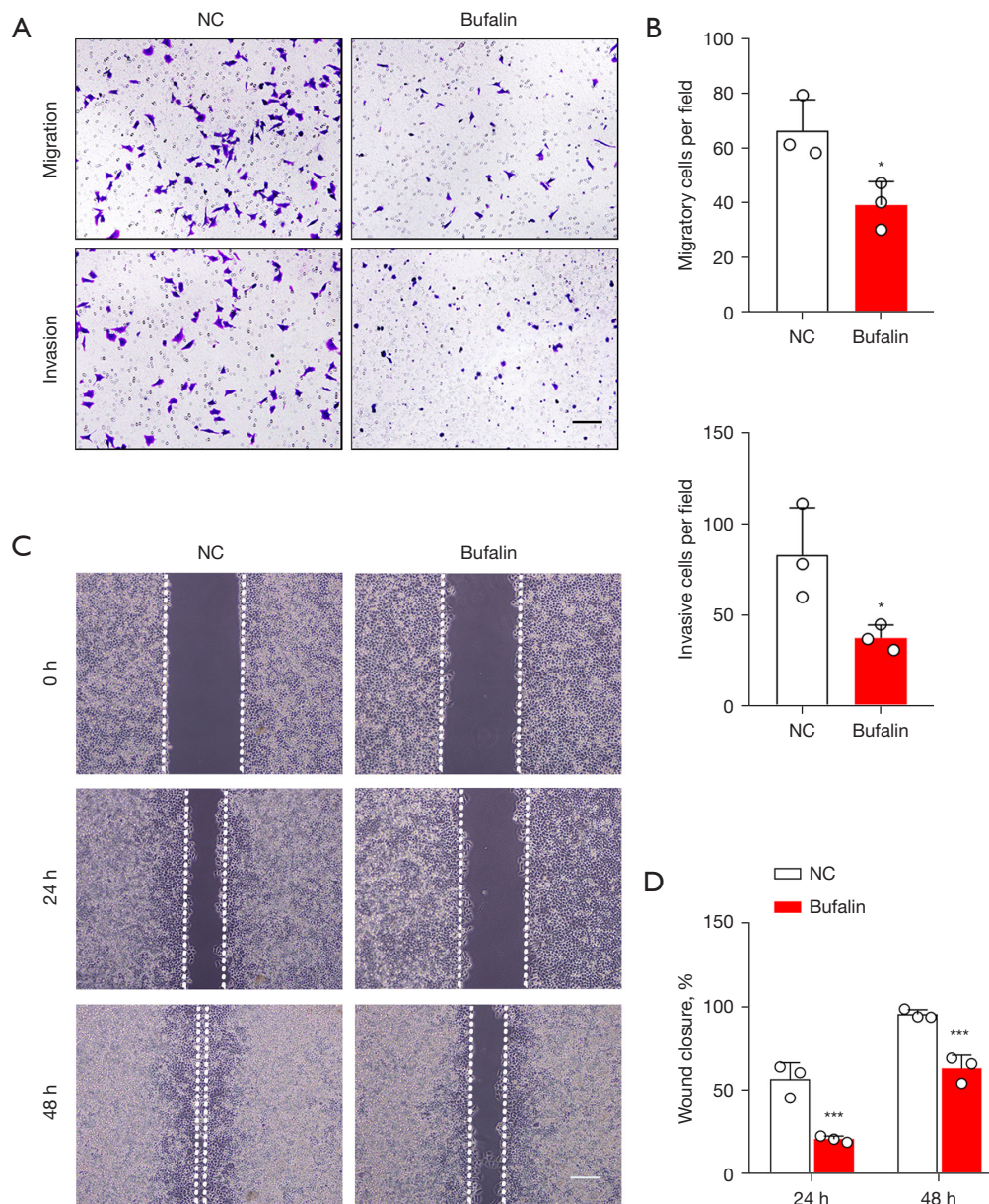
Figure 2 Bufalin inhibits migration and invasion of ECA109 cells. (A) The effect of Bufalin on cell migration and invasion of ECA109 cells was investigated by transwell assay (crystal violet staining, scale bar =500 µm). (B) The statistics result of transwell assay. (C)The effect of Bufalin on cell migration of ECA109 cells was investigated by wound healing assay (scale bar =100 µm). (D) The statistics result of wound healing assay. Data are presented as mean ± SD (error bars). Statistical significance was tested by unpaired Student's *t*-test. *, P<0.05; ***, P<0.001. NC, negative control; SD, standard deviation.

in the Bufalin group was significantly reduced compared to that of the NC group (P<0.05) (*Figure 2A,2B*), and the scratch healing ability was significantly reduced (P<0.01) (*Figure 2C,2D*). These findings suggest that Bufalin inhibited the migration and invasion of ECA109 cells. Thus, Bufalin appears to inhibit the proliferation, migration, and invasion

of the ECA109 cells.

Bufalin inhibits the proliferation, migration, and invasion of the ECA109 cells through the PIAS3

To further explore the mechanism of Bufalin-mediated
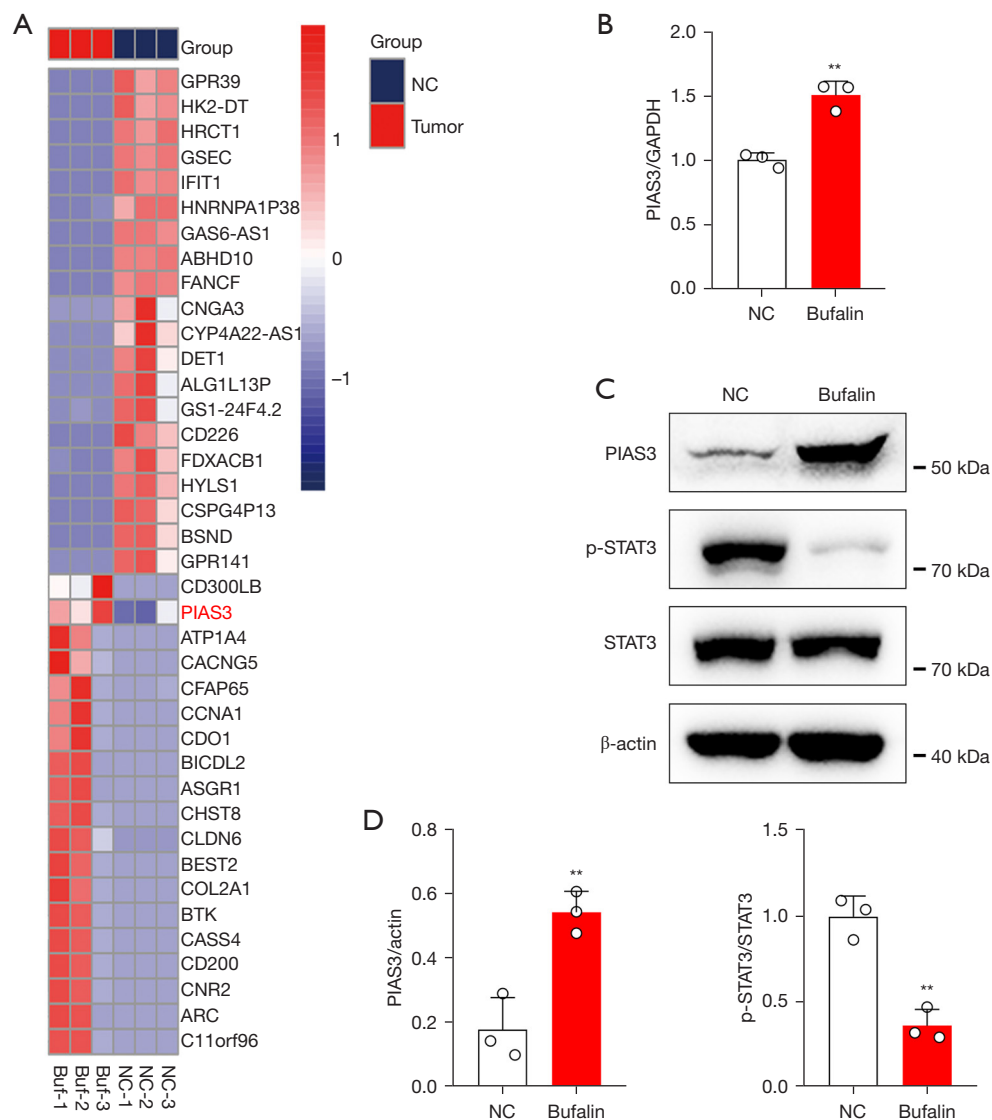
Figure 3 Bufalin inhibits the JAK-STAT3 signaling pathway in ECA109 cells. (A) ECA109 cells were treated with 200 nM Bufalin for 24 h. ECA109 cells were divided into NC group and Bufalin group. Each group had three replicates, and labeled as NC-1, NC-2, NC-3 and Buf-1, Buf-2, Buf-3. The total RNA of ECA109 cells was used for RNA-seq analysis. Heatmaps of differentially expressed genes were shown based on results from RNA-seq (log2 scale). (B) The expressions of PIAS3 in ECA109 cells of Bufalin group and NC group were measured by qRT-PCR. (C) The expressions of PIAS3, p-STAT3 and STAT3 in ECA109 cells of Bufalin group and NC group were measured by Western blot. β-actin was used as an internal control. (D) The statistics result of Western blot. Data are presented as mean ± SD (error bars). Statistical significance was tested by unpaired Student's *t*-test. **, P<0.01. GAPDH, glyceraldehyde-3-phosphate dehydrogenase; NC, negative control; Buf, Bufalin; p, phosphorylated; PIAS3, protein inhibitor of activated signal transducer and activator of transcription 3; STST3, signal transducer and activator of transcription 3; qRT-PCR, quantitative real-time polymerase chain reaction; RNA-seq, RNA-sequencing; SD, standard deviation.

anti-tumor function, total RNA was extracted from the ECA109 cells of the NC and Bufalin groups and RNA-seq was performed. The results showed that the expression of the anti-tumor gene PIAS3 was significantly increased after Bufalin treatment (*Figure 3A*). PIAS3 has been shown to bind to STAT3 directly and inactivate it, thereby inhibiting

its induced gene transcription. The overexpression of STAT3 caused by the loss of PIAS3 may promote the growth and proliferation of tumor cells. Tumor occurrence and metastasis are closely related to the Janus kinase 2 (JAK2)-STAT3 signal transduction pathway. The JAK-STAT signaling pathway is an information chain in cells that regulates protein interactions and participates in immunity, cell division, cell death, tumor formation, development, invasion, and metastasis (42). The activation of the STAT3 signaling pathway contributes to the formation of the tumor inflammatory microenvironment, participates in tumor angiogenesis, epithelial mesenchymal transformation, and extracellular matrix degradation, and plays an important role in tumor invasion and metastasis. Based on the above RNA-seq results, we further confirmed that Bufalin upregulates the expression of PIAS3 in the ECA109 cells by qRT-PCR and Western blot analysis. Additionally, the expression of p-STAT3 was significantly decreased, while the expression of total STAT3 did not change significantly (*Figure 3B-3D*). These results indicate that Bufalin may inhibit the proliferation, migration, and invasion of the ECA109 cells by inhibiting the STAT3 signaling pathway.

PIAS3 inhibits the proliferation, migration, and invasion of ECA109 cells

PIAS3 may play different roles in the development of different types of tumors. To further explore the role of PIAS3 in the development of EC, we first detected its expression in ESCC. The IHC detection results showed that the expression level of PIAS3 in the ESCC tissues was significantly lower than that in the corresponding adjacent tissues (*Figure 4A*). The Western blot results further confirmed that the expression level of PIAS3 in the ESCC tissues was significantly lower than that in the corresponding adjacent tissues ($P<0.05$) (*Figure 4B,4C*). In addition, we analyzed PIAS3 expression in the tumor samples and their adjacent normal tissue samples using the RNA-seq results from The Cancer Genome Atlas database (https://tcga-data.nci.nih.gov/tcga/). Consistent with the detection results, PIAS3 mRNA expression was downregulated in the ESCC tumor tissues ($P<0.05$) (*Figure 4D*).

Next, we examined the effects of PIAS3 on the proliferation, migration, and invasion of the ECA109 cells. First, PIAS3 siRNAs were transfected into the ECA109 cells to knockdown the expression of PIAS3. The transfection efficiency is shown in *Figure 5A-5C*. Among the 3 siRNAs, siRNA-2# had the best knockdown effect,

and was thus chosen for PIAS3 knockdown in the following experiments. Subsequently, the effects of Bufalin on the proliferation of the ECA109 cells were detected by CCK-8 and EdU assays. The results showed that the knockdown of PIAS3 significantly enhanced the proliferation of the ECA109 cells (*Figure 5D-5F*). In addition, to examine the effects of PIAS3 on the migration and invasion of ECA109 cells, we conducted wound-healing and transwell assays. The results showed that the number of transmembrane cells in the PIAS3 siRNA-2# group was significantly increased compared to that of the NC group ($P<0.05$) (*Figure 6A,6B*), and the scratch healing ability was significantly enhanced ($P<0.01$) (*Figure 6C,6D*). These findings showed that PIAS3 inhibits the proliferation, migration, and invasion of ECA109 cells.

Bufalin inhibits the proliferation, migration, and invasion of ECA109 cells by upregulating PIAS3 to inhibit the STAT3 signaling pathway

The above findings indicate that the expression of PIAS3 is regulated by Bufalin. Next, we sought to determine whether the loss of PIAS3 could reverse the tumor suppressor effects induced by Bufalin. After PIAS3 was reduced in the ECA109 cells, the anti-cancer effects, including cell growth (*Figure 7*), migration, and invasion (*Figure 8A-8D*) of Bufalin were partially impaired. In addition, after PIAS3 expression was decreased, the expression of p-STAT3 in Bufalin + PIAS3 siRNA-2# group was increased compared to Bufalin group, which partially reversed the inhibition of Bufalin, but the total expression of STAT3 did not change (*Figure 8E,8F*). In conclusion, these results indicate that Bufalin inhibits the proliferation, migration, and invasion of the ECA109 cells by upregulating PIAS3 to inhibit the STAT3 signaling pathway.

Discussion

EC is a common malignant tumor of the digestive tract, and its morbidity and mortality are very high. At present, surgical resection, chemotherapy, and radiotherapy are still the main treatments for EC. The chemotherapeutic drugs for the treatment of EC have some limitations. Notably, the side effects of the drugs are serious, and the therapeutic effects are not ideal. In recent years, the potential use of TCM in the treatment of tumors has received widespread attention and shown certain clinical advantages (9,11). Notably, TCM has been shown to
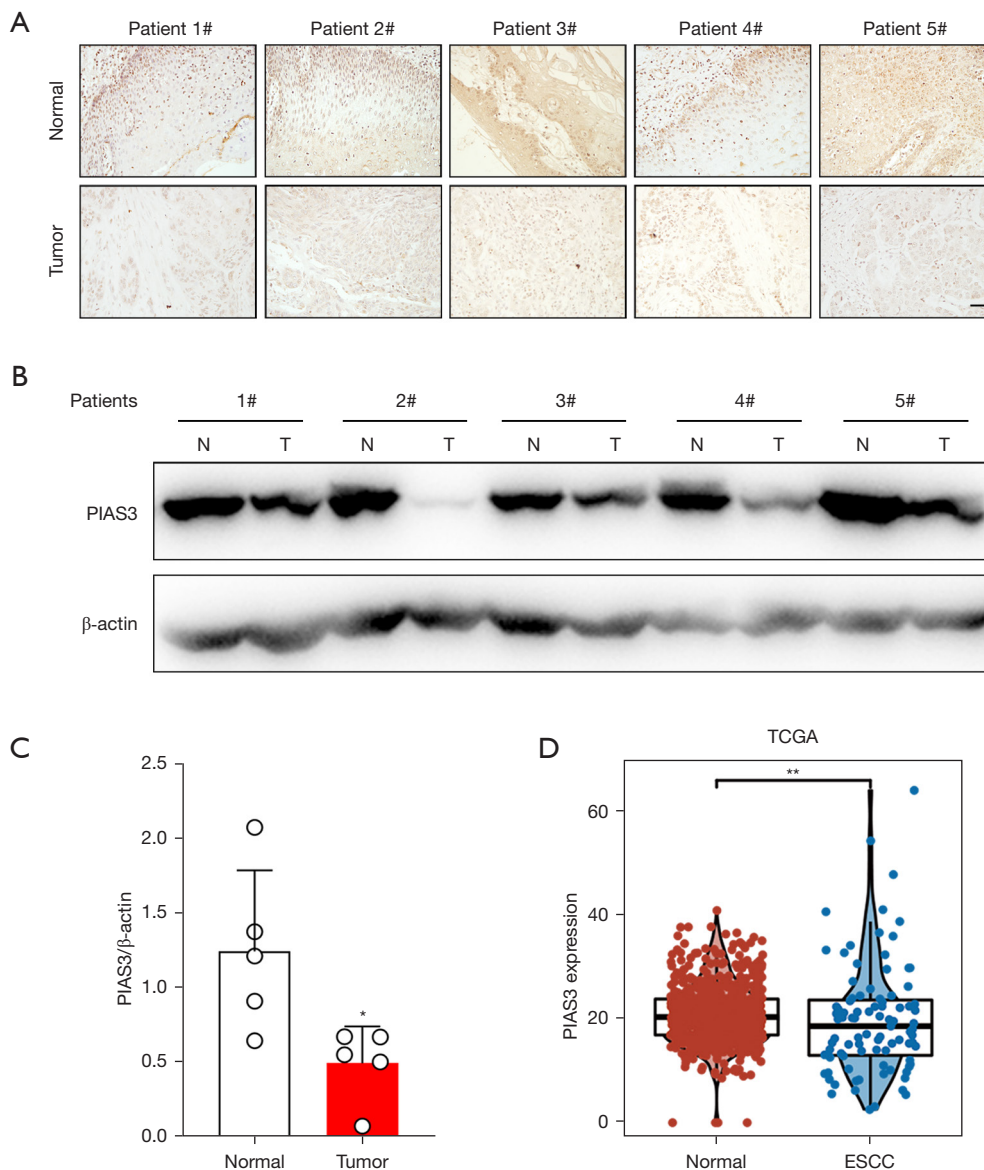
Figure 4 PIAS3 is downregulated in ESCC. (A) IHC staining of PIAS3 expression in human ESCC and normal esophageal tissues (scale bar =200 μm). (B) Western blot analysis was performed to detect the expression of PIAS3 in human ESCC and normal esophageal tissues (n=5). (C) The statistics result of Western blot. (D) Analysis of PIAS3 gene expression in ESCC and adjacent normal tissues in TCGA database. Data are presented as mean ± SD (error bars). Statistical significance was tested by unpaired Student's t-test. *, $P<0.05$; **, $P<0.01$. ESCC, esophageal squamous cell carcinoma; IHC, immunohistochemistry; N, normal; T, tumor; PIAS3, protein inhibitor of activated signal transducer and activator of transcription 3; TCGA, The Cancer Genome Atlas; qRT-PCR, quantitative real-time polymerase chain reaction; SD, standard deviation.

improve the postoperative immunity of patients, reduce the side effects of radiotherapy and chemotherapy, inhibit tumor recurrence, and reduce metastasis (9). For example, Oridonin was shown to inhibit the proliferation of EC cells by inducing apoptosis and blocking cells in the G2/M phase

(43,44). TCM also has been shown to inhibit the migration of EC cells by inhibiting the expression of epithelial-interstitial transition markers (45). Some types of TCM significantly inhibit cancer cell proliferation and metastasis. For example, the injection of compound *Sophora flavescens*
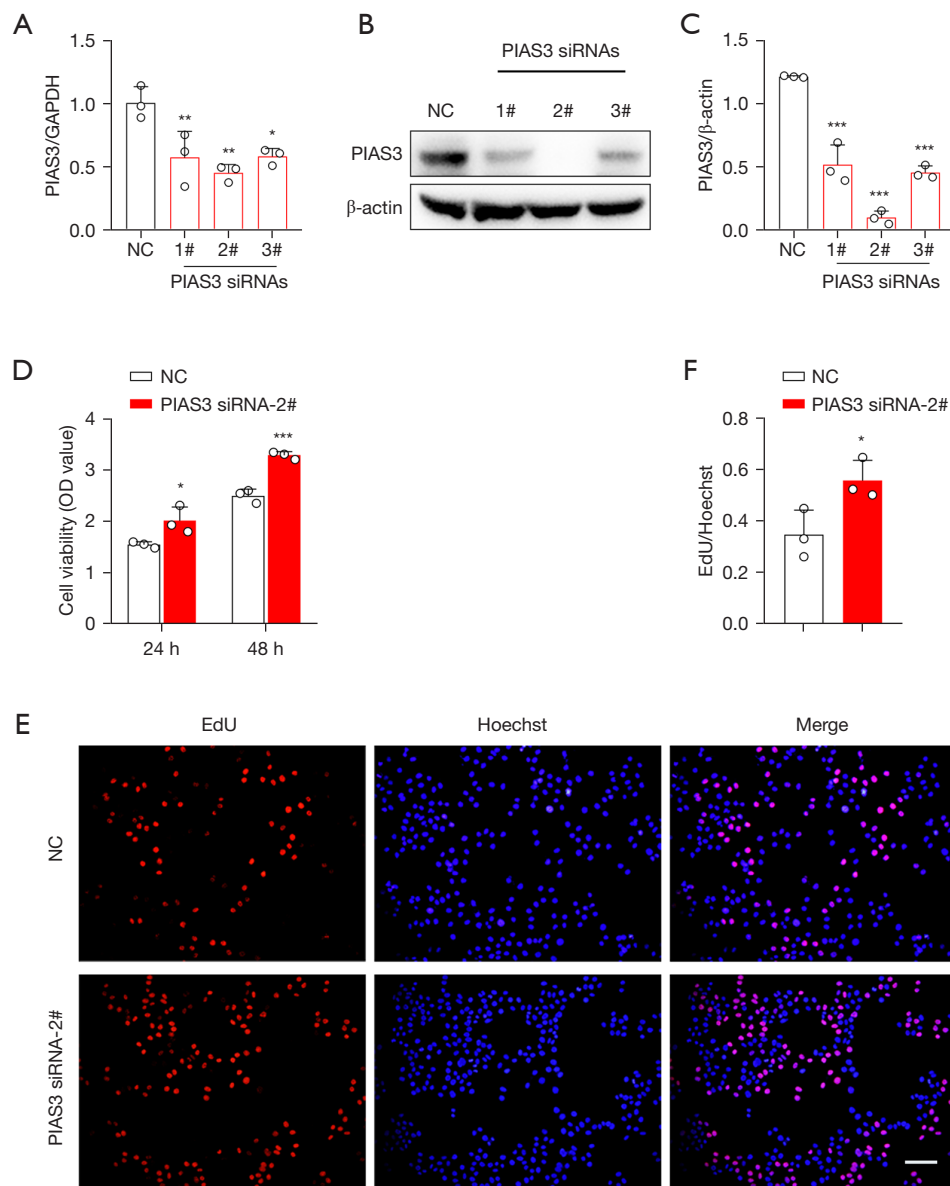
Figure 5 PIAS3 inhibits proliferation of ECA109 cells. (A) ECA109 cells were transfected with PIAS3 siRNAs for 48 h. PIAS3 mRNA levels was detected by qRT-PCR. GAPDH was used for normalization of the gene expression. (B) ECA109 cells were transfected with PIAS3 siRNAs for 48 h. PIAS3 protein levels was detected by Western blot. β-actin was used as an internal control. (C) The statistics result of Western blot. ECA109 cells were transfected with PIAS3 siRNAs for 48 h. The effect of PIAS3 on cell proliferation was measured by CCK-8 assay (D) and EdU assay (E) (scale bar =500 µm). (F) The statistics result of EdU assay. Data are presented as mean ± SD (error bars). Statistical significance was tested by unpaired Student's *t*-test. *, P<0.05; **, P<0.01; ***, P<0.001. CCK-8, Cell Counting Kit-8; EdU, 5-ethynyl-2'-deoxyuridine; GAPDH, glyceraldehyde-3-phosphate dehydrogenase; NC, negative control; OD, optical density; PIAS3, protein inhibitor of activated signal transducer and activator of transcription 3; qRT-PCR, quantitative real-time polymerase chain reaction; SD, standard deviation.
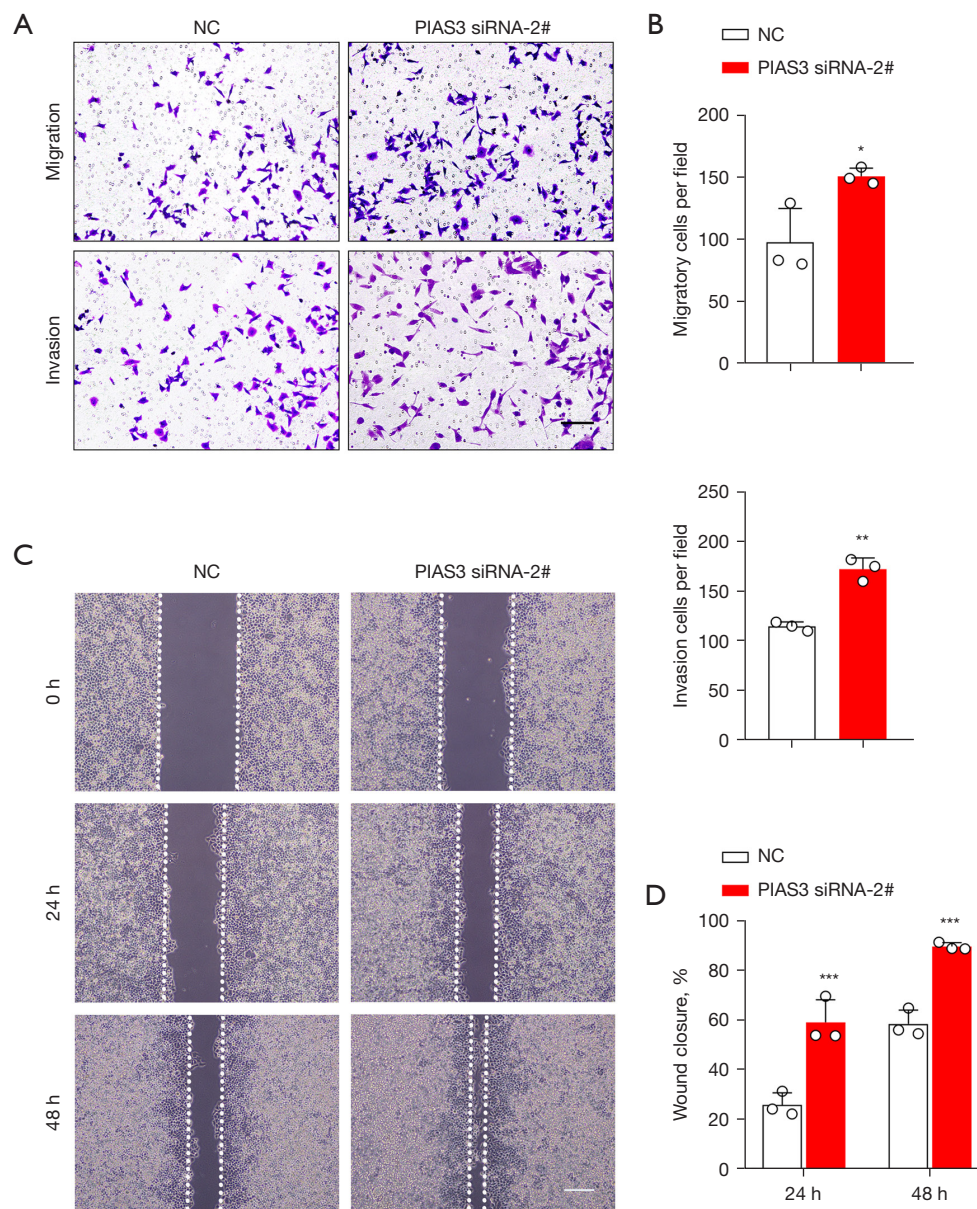
Figure 6 PIAS3 inhibits migration and invasion of ECA109 cells. (A) The effect of PIAS3 on cell migration and invasion of ECA109 cells was investigated by transwell assay (crystal violet staining, scale bar =500 μm). (B) The statistics result of transwell assay. (C) The effect of PIAS3 on cell migration of ECA109 cells was investigated by wound healing assay (scale bar =100 μm). (D) The statistics result of wound healing assay. Data are presented as mean ± SD (error bars). Statistical significance was tested by unpaired Student's t-test. *, P<0.05; **, P<0.01; ***, P<0.001. NC, negative control; PIAS3, protein inhibitor of activated signal transducer and activator of transcription 3; SD, standard deviation.

has been shown to effectively inhibit the metastasis of colon cancer, brain cancer, and breast cancer (46), ginsenoside has been shown to inhibit the metastasis of gastric cancer cells (47,48), and triptolide has been shown to significantly inhibit the proliferation of cervical cancer Hela cells *in vitro*.

The mechanism of anti-proliferation is related to cell cycle arrest in the S phase, which affects the expression of cyclin B1 and changes the phosphorylation of P34 (49,50).

Bufalin is an antitumor active ingredient extracted from the TCM Venenum Bufonis. Bufalin has anti-tumor,
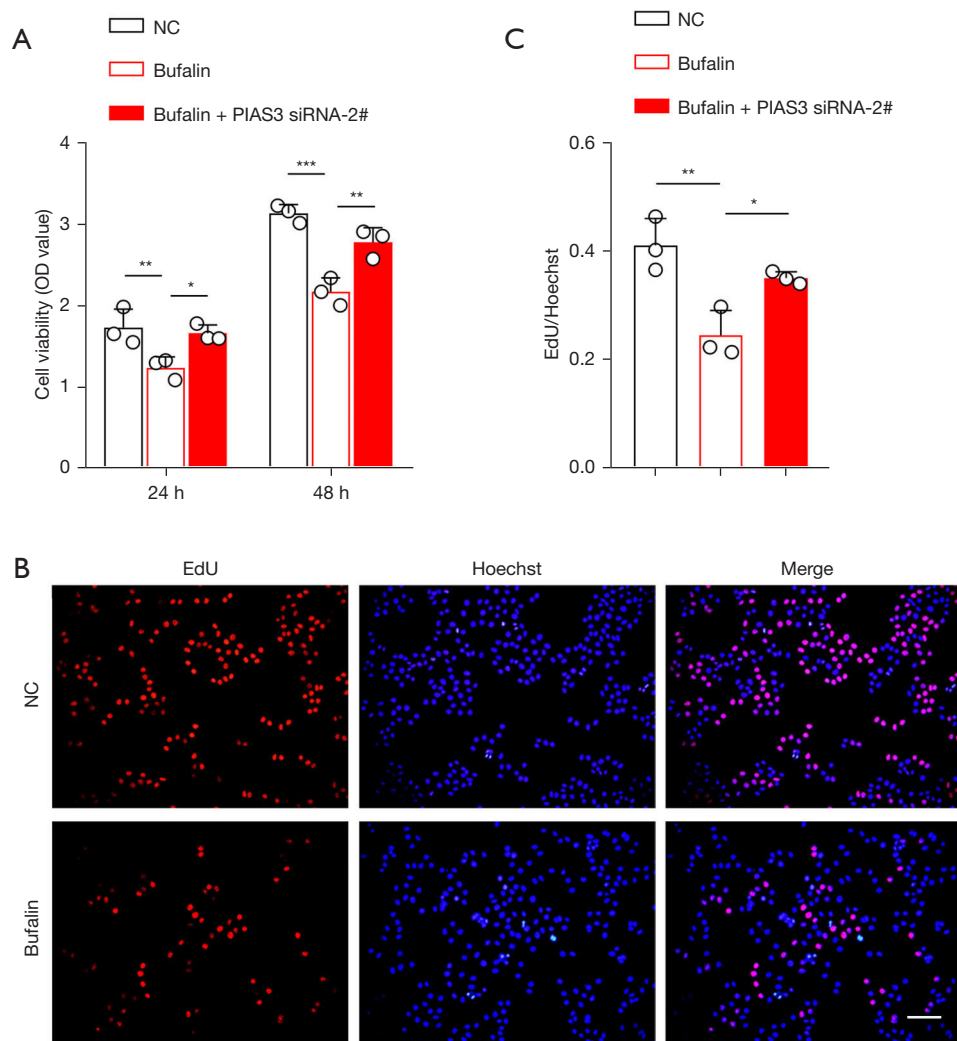
Figure 7 PIAS3 knockdown partially rescues inhibited cell proliferation induced by Bufalin. ECA109 cells were transfected with PIAS3 siRNA-2# for 48 h, and then treated with 200 nM Bufalin for another 24 h. Cell proliferation was measured by CCK-8 assay (A) and EdU assay (B) (scale bar =500 µm). (C) The statistics result of EdU assay. Data are presented as mean ± SD (error bars). Statistical significance was tested by unpaired Student's *t*-test. *, P<0.05; **, P<0.01; ***, P<0.001. CCK-8, Cell Counting Kit-8; EdU, 5-ethynyl-2'-deoxyuridine; NC, negative control; OD, optical density; PIAS3, protein inhibitor of activated signal transducer and activator of transcription 3; SD, standard deviation.

diuretic, cardiotonic, hypertensive, local anesthetic, anti-inflammatory, anti-radiation, and anti-tussive effects and inhibits Na^+/K^+-ATPase (51,52). In the aspect of anti-tumor, Bufalin can inhibit the growth of tumor cells, promote the differentiation of tumor cells and induce the apoptosis of tumor cells (53). Bufalin can inhibit tumor cell proliferation by blocking phosphatidylinositol-3-kinase/serine protein kinase signal pathway, and induce tumor cell apoptosis through mitochondrial or death receptor-mediated pathway (54), which can reverse the drug resistance of hepatocellular carcinoma cells to fluorouracil (22). Qi *et al.* showed that Bufalin could induce apoptosis of hepatocellular carcinoma HepG2 cells through Fas-mediated Caspase-10 pathway (55). Xie *et al.* found that Bufalin can induce colon cancer cells to activate autophagy through N-terminal kinase [c-Jun N-terminal kinase (JNK)] pathway, resulting in autophagic apoptosis (56). It has been found that Bufalin can effectively inhibit the metastasis
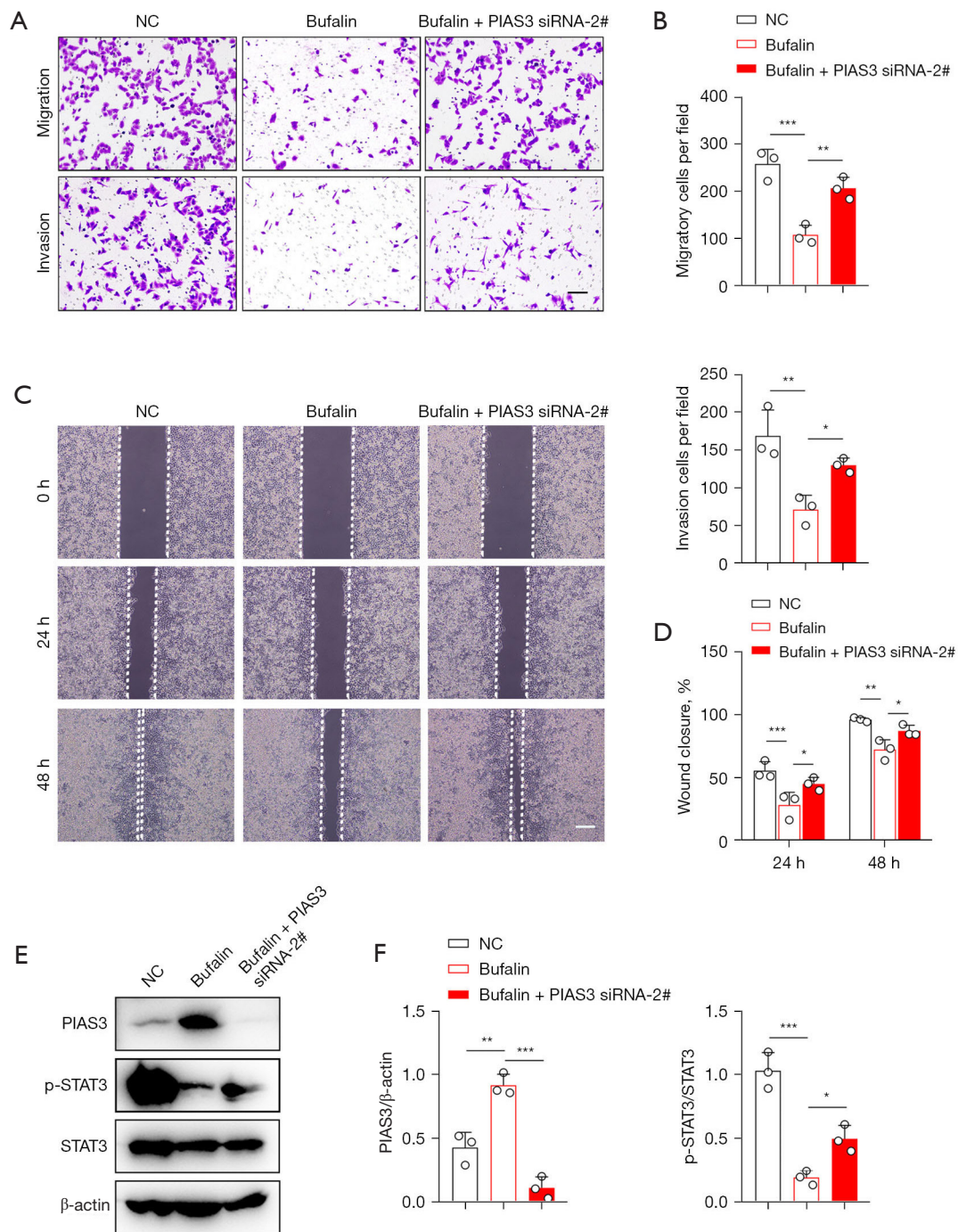
Figure 8 PIAS3 knockdown partially rescues inhibited cell migration and invasion induced by Bufalin. ECA109 cells were transfected with PIAS3 siRNA-2# for 48 h, and then treated with 200 nM Bufalin for another 24 h. Cell migration and invasion was measured by transwell assay (A) (crystal violet staining, scale bar =500 µm) and wound healing assay (C) (scale bar =100 µm). (B) The statistics result of transwell assay. (D) The statistics result of wound healing assay. (E) The expressions of PIAS3, p-STAT3 and STAT3 in ECA109 cells of NC, Bufalin and Bufalin + PIAS3 siRNA-2# groups were measured by Western blot. β-actin was used as an internal control. (F) The statistics result of Western blot. Data are presented as mean ± SD (error bars). Statistical significance was tested by unpaired Student's t-test. *, P<0.05; **, P<0.01; ***, P<0.001. NC, negative control; p, phosphorylated; PIAS3, protein inhibitor of activated signal transducer and activator of transcription 3; STST3, signal transducer and activator of transcription 3; SD, standard deviation.

of lung cancer NCI-H460 cells, which may be related to the inhibition of matrix metalloproteinase-9 (MMP-9) activity, the decrease of cytoplasmic NF-κB production and the reduction of NF-κB nuclear translocation (57). Hong *et al.* found that Bufalin can inhibit the invasion and migration of bladder cancer cells, the mechanism is that it can inhibit the invasiveness of bladder cancer cells by reducing blocking protein, increasing transmembrane resistance and tightening tight junction, and inhibit its migration by activating ERK pathway and inactivating matrix metalloproteinase-2 (MMP-2) and MMP-9 (58). Qiu *et al.* found that, Bufalin combined with mir-497 could inhibit the expression of vascular endothelial growth factor [vascular endothelial growth factor (VEGFA)], inhibit the metastasis of neovascularization colorectal cancer and improve the quality of life of experimental animals (59). Bufalin could inhibit the proliferation, migration, invasion and adhesion of hepatoma cells. The main mechanism was that Bufalin significantly decreased the levels of p-AKT, p-GSK-3β, MMP-9 and MMP-2, increased the expression of GSK-3β and E-cadherin, and inhibited the nuclear translocation of β-catenin (60). The above studies show that Bufalin can inhibit the proliferation, migration and apoptosis of tumor cells in many ways. In this study, we found that Bufalin not only inhibited the proliferation, migration, and invasion of the ECA109 cells *in vitro*, but also inhibited the tumorigenesis and growth of the ECA109 cells *in vivo*. Subsequently, we detected the differentially expressed genes before and after Bufalin treatment. The RNA-seq results showed that the expression of PIAS3 was significantly increased after Bufalin treatment. Research confirms that miRNA-21 is a novel miRNA regulating immune cell recruitment, which acts at least in part via its inhibition of PIAS3 expression and oncogenic STAT3 signalling in tumour cells (61). Roberts have confirmed that PIAS3 can bind to the rPP-C8 region of STAT3 and block JAK/STAT signal pathway, which can inhibit the proliferation of tumor cells and promote apoptosis (62). In the PI3K/AKT signal pathway, PIAS3 can inhibit the phosphorylation of Akt and inactivate the signal pathway, thus inhibiting the proliferation and division of tumor cells (37).

The regulation factor of STAT3 is very important for the regulation of STAT3 effect intensity and duration after STAT3 is activated by the JAK pathway. Researchers have found that a variety of factors regulate the activation of STAT3, among which PIAS3 has been studied extensively. PIAS3 has been proven to bind directly to STAT3

and inactivate it, thus inhibiting STAT3 induced gene transcription (63,64). However, the direct inactivation of STAT3 by PIAS3 can be reversed by the direct interaction between the zinc finger protein Gfi-1 and PIAS3 (65). Sun *et al.* showed that PIAS3 was also involved in the dephosphorylation of activated STAT3 (63). It has been suggested that the overexpression of STAT3 caused by the loss of PIAS3 expression may promote the growth and proliferation of tumor cells (66), while enhancing the expression of PIAS3 causes some types of tumor cells to grow and restores their drug sensitivity (37). In this study, we found that the positive expression of PIAS3 in the tumor tissues of the ESCC patients was significantly lower than that in the adjacent tissues. Moreover, the protein level of PIAS3 in the tumor tissues was also significantly lower than that in the adjacent tissues. After PIAS3 knockdown, the proliferation, migration, and invasion abilities of the ECA109 cells were significantly improved. Thus, PIAS3 deletion may play an important role in the evolution and development of ESCC.

Bufalin increased the expression level of PIAS3 and decreased the expression level of p-STAT3 in the ECA109 cells after 24 h of treatment. The anti-tumor effects of Bufalin were further verified by the *in vivo* anti-tumor experiment in the nude mice. The nude mice were inoculated with normal ECA109 cells. After Bufalin treatment, the tumor volume was decreased in Bufalin group compared to the NC group, and the tumor growth was slowed down in Bufalin group. To examine the relationship between the anti-tumor effects of Bufalin and the PIAS3/STAT3 signaling pathway, we first knocked down the expression of PIAS3 in the ECA109 cells by siRNA, and then treated the cells with 200 nM of Bufalin. We found that PIAS3 knockdown partially reversed the inhibitory effects of Bufalin on the tumor cells, and the expression of p-STAT3 was increased. Thus, the proliferation, migration, and invasion of the tumor cells were inhibited by upregulating the activity of PIAS3, inhibiting STAT3, and downregulating the expression of p-STAT3. The results provide an experimental basis for the clinical application of Bufalin in the treatment of ESCC.

Conclusions

Taken together, we found that Bufalin inhibited the proliferation, migration, and invasion of ECA109 cells. Bufalin also had obvious inhibitory effects on the transplanted tumors of the ECA109 cells in the nude

mice. In addition, we also found that Bufalin may inhibit the proliferation, migration, and invasion of the ECA109 cells, upregulate the activity of PIAS3, inhibit STAT3, and downregulate the expression of p-STAT3. Bufalin had anti-tumor effects on the ECA109 cells. Further research on the role and molecular mechanism of Bufalin in ESCC and other malignant tumors will provide a more reliable basis for the application of Bufalin in clinical tumor therapy.

Acknowledgments

Footnote

Reporting Checklist: The authors have completed the MDAR and ARRIVE reporting checklists. Available at https://jtd.amegroups.com/article/view/10.21037/jtd-23-486/rc

Data Sharing Statement: Available at https://jtd.amegroups.com/article/view/10.21037/jtd-23-486/dss

Peer Review File: Available at https://jtd.amegroups.com/article/view/10.21037/jtd-23-486/prf

Conflicts of Interest: All authors have completed the ICMJE uniform disclosure form (available at https://jtd.amegroups.com/article/view/10.21037/jtd-23-486/coif). QS, CL, and GF are employees from Zhongke Gene Biotechnology. The other authors have no conflicts of interest to declare.

Ethical Statement: The authors are accountable for all aspects of the work in ensuring that questions related to the accuracy or integrity of any part of the work are appropriately investigated and resolved. The study was conducted in accordance with the Declaration of Helsinki (as revised in 2013). The collection of all the ESCC specimens was approved by the Ethics Committee of Shanghai Tenth People's Hospital (No. SHSY-IEC-4.1/21-78/02), and the informed consent of patients was obtained. Animal experiments were performed under a project license (No. S20200323-186) granted by Institutional Animal Care and Use Committees of the Nantong University, in compliance with the institutional guidelines for the care and use of animals.

Open Access Statement: This is an Open Access article distributed in accordance with the Creative Commons Attribution-NonCommercial-NoDerivs 4.0 International License (CC BY-NC-ND 4.0), which permits the non-commercial replication and distribution of the article with the strict proviso that no changes or edits are made and the original work is properly cited (including links to both the formal publication through the relevant DOI and the license). See: https://creativecommons.org/licenses/by-nc-nd/4.0/.

References

1. Dupuis O, Ganem G, Béra G, et al. Esophageal cancer. Cancer Radiother 2010;14 Suppl 1:S74-S83.
2. Morgan E, Soerjomataram I, Rumgay H, et al. The Global Landscape of Esophageal Squamous Cell Carcinoma and Esophageal Adenocarcinoma Incidence and Mortality in 2020 and Projections to 2040: New Estimates From GLOBOCAN 2020. Gastroenterology 2022;163:649-658.e2.
3. Ying J, Huang HH, Zhang MM, et al. Up-regulation of SOCS4 promotes cell proliferation and migration in esophageal squamous cell carcinoma. Transl Cancer Res 2021;10:2416-27.
4. Zhou J, Zheng R, Zhang S, et al. Gastric and esophageal cancer in China 2000 to 2030: Recent trends and short-term predictions of the future burden. Cancer Med 2022;11:1902-12.
5. Glenn TF. Esophageal cancer. Facts, figures, and screening. Gastroenterol Nurs 2001;24:271-3; quiz 274-5.
6. Lagergren J, Smyth E, Cunningham D, et al. Oesophageal cancer. Lancet 2017;390:2383-96.
7. Jayaprakasam VS, Yeh R, Ku GY, et al. Role of Imaging in Esophageal Cancer Management in 2020: Update for Radiologists. AJR Am J Roentgenol 2020;215:1072-84.
8. Yang YX, Zheng YZ, Gao TT, et al. Progression-free survival at 3 years is a reliable surrogate for 5-year overall survival for patients suffering from locally advanced esophageal squamous cell carcinoma. Cancer Med 2022;11:3751-60.
9. Xiang Y, Guo Z, Zhu P, et al. Traditional Chinese medicine as a cancer treatment: Modern perspectives of ancient but advanced science. Cancer Med 2019;8:1958-75.
10. Wang Y, Zhang Q, Chen Y, et al. Antitumor effects of immunity-enhancing traditional Chinese medicine. Biomed Pharmacother 2020;121:109570.
11. Zhang Y, Lou Y, Wang J, et al. Research Status and Molecular Mechanism of the Traditional Chinese

Medicine and Antitumor Therapy Combined Strategy Based on Tumor Microenvironment. Front Immunol 2020;11:609705.

12. Soumoy L, Ghanem GE, Saussez S, et al. Bufalin for an innovative therapeutic approach against cancer. Pharmacol Res 2022;184:106442.

13. Zhang JJ, Zhou XH, Zhou Y, et al. Bufalin suppresses the migration and invasion of prostate cancer cells through HOTAIR, the sponge of miR-520b. Acta Pharmacol Sin 2019;40:1228-36.

14. Yu CH, Kan SF, Pu HF, et al. Apoptotic signaling in bufalin- and cinobufagin-treated androgen-dependent and -independent human prostate cancer cells. Cancer Sci 2008;99:2467-76.

15. Yu Z, Li Y, Li Y, et al. Bufalin stimulates antitumor immune response by driving tumor-infiltrating macrophage toward M1 phenotype in hepatocellular carcinoma. J Immunother Cancer 2022;10:e004297.

16. Ye M, Tang Y, He J, et al. Alisol B 23-Acetate Increases the Antitumor Effect of Bufalin on Liver Cancer through Inactivating Wnt/β-Catenin Axis. Comput Math Methods Med 2022;2022:6249534.

17. Wang J, Cai H, Xia Y, et al. Bufalin inhibits gastric cancer invasion and metastasis by down-regulating Wnt/ASCL2 expression. Oncotarget 2018;9:23320-33.

18. Qi HY, Qu XJ, Liu J, et al. Bufalin induces protective autophagy by Cbl-b regulating mTOR and ERK signaling pathways in gastric cancer cells. Cell Biol Int 2019;43:33-43.

19. Dou L, Zou D, Song F, et al. Bufalin suppresses ovarian cancer cell proliferation via EGFR pathway. Chin Med J (Engl) 2021;135:456-61.

20. Shih YL, Chou JS, Chen YL, et al. Bufalin Enhances Immune Responses in Leukemic Mice Through Enhancing Phagocytosis of Macrophage In Vivo. In Vivo 2018;32:1129-36.

21. Zhai B, Hu F, Yan H, et al. Bufalin Reverses Resistance to Sorafenib by Inhibiting Akt Activation in Hepatocellular Carcinoma: The Role of Endoplasmic Reticulum Stress. PLoS One 2015;10:e0138485.

22. Gu W, Liu L, Fang FF, et al. Reversal effect of bufalin on multidrug resistance in human hepatocellular carcinoma BEL-7402/5-FU cells. Oncol Rep 2014;31:216-22.

23. Zhao H, Li Q, Pang J, et al. Blocking autophagy enhances the pro-apoptotic effect of bufalin on human gastric cancer cells through endoplasmic reticulum stress. Biol Open 2017;6:1416-22.

24. Hu F, Han J, Zhai B, et al. Blocking autophagy enhances

the apoptosis effect of bufalin on human hepatocellular carcinoma cells through endoplasmic reticulum stress and JNK activation. Apoptosis 2014;19:210-23.

25. Lian X, Wang H, Wei X, et al. BMI-1 is important in bufalin-induced apoptosis of K562 cells. Mol Med Rep 2014;9:1209-17.

26. Huang AC, Yang MD, Hsiao YT, et al. Bufalin inhibits gefitinib resistant NCI-H460 human lung cancer cell migration and invasion in vitro. J Ethnopharmacol 2016;194:1043-50.

27. Tian X, Dai S, Sun J, et al. Bufalin Induces Mitochondria-Dependent Apoptosis in Pancreatic and Oral Cancer Cells by Downregulating hTERT Expression via Activation of the JNK/p38 Pathway. Evid Based Complement Alternat Med 2015;2015:546210.

28. Amano Y, Cho Y, Matsunawa M, et al. Increased nuclear expression and transactivation of vitamin D receptor by the cardiotonic steroid bufalin in human myeloid leukemia cells. J Steroid Biochem Mol Biol 2009;114:144-51.

29. Jiang L, Zhao MN, Liu TY, et al. Bufalin induces cell cycle arrest and apoptosis in gallbladder carcinoma cells. Tumour Biol 2014;35:10931-41.

30. Hsu CM, Tsai Y, Wan L, et al. Bufalin induces G2/M phase arrest and triggers autophagy via the TNF, JNK, BECN-1 and ATG8 pathway in human hepatoma cells. Int J Oncol 2013;43:338-48.

31. Ji D, Liang Z, Liu G, et al. Bufalin attenuates cancer-induced pain and bone destruction in a model of bone cancer. Naunyn Schmiedebergs Arch Pharmacol 2017;390:1211-9.

32. Liu Y, Wang X, Jia Y, et al. Effects of bufalin on the mTOR/p70S6K pathway and apoptosis in esophageal squamous cell carcinoma in nude mice. Int J Mol Med 2017;40:357-66.

33. Zhang J, Zhang Y, Ma Y, et al. Therapeutic Potential of Exosomal circRNA Derived from Synovial Mesenchymal Cells via Targeting circEDIL3/miR-485-3p/PIAS3/STAT3/VEGF Functional Module in Rheumatoid Arthritis. Int J Nanomedicine 2021;16:7977-94.

34. Chen S, Dong Z, Cheng M, et al. Homocysteine exaggerates microglia activation and neuroinflammation through microglia localized STAT3 overactivation following ischemic stroke. J Neuroinflammation 2017;14:187.

35. Zhang C, Mukherjee S, Tucker-Burden C, et al. TRIM8 regulates stemness in glioblastoma through PIAS3-STAT3. Mol Oncol 2017;11:280-94.

36. Abbas R, McColl KS, Kresak A, et al. PIAS3 expression

in squamous cell lung cancer is low and predicts overall survival. Cancer Med 2015;4:325-32.

37. Ogata Y, Osaki T, Naka T, et al. Overexpression of PIAS3 suppresses cell growth and restores the drug sensitivity of human lung cancer cells in association with PI3-K/Akt inactivation. Neoplasia 2006;8:817-25.

38. Jiang M, Zhang W, Zhang R, et al. Cancer exosome-derived miR-9 and miR-181a promote the development of early-stage MDSCs via interfering with SOCS3 and PIAS3 respectively in breast cancer. Oncogene 2020;39:4681-94.

39. Chandhoke AS, Chanda A, Karve K, et al. The PIAS3-Smurf2 sumoylation pathway suppresses breast cancer organoid invasiveness. Oncotarget 2017;8:21001-14.

40. Tseng JC, Huang SH, Lin CY, et al. ROR2 suppresses metastasis of prostate cancer via regulation of miR-199a-5p-PIAS3-AKT2 signaling axis. Cell Death Dis 2020;11:376.

41. Polimeno L, Francavilla A, Piscitelli D, et al. The role of PIAS3, p-STAT3 and ALR in colorectal cancer: new translational molecular features for an old disease. Eur Rev Med Pharmacol Sci 2020;24:10496-511.

42. O'Shea JJ, Schwartz DM, Villarino AV, et al. The JAK-STAT pathway: impact on human disease and therapeutic intervention. Annu Rev Med 2015;66:311-28.

43. Jiang JH, Pi J, Jin H, et al. Oridonin-induced mitochondria-dependent apoptosis in esophageal cancer cells by inhibiting PI3K/AKT/mTOR and Ras/Raf pathways. J Cell Biochem 2019;120:3736-46.

44. Zhang J, Wang N, Zhou Y, et al. Oridonin induces ferroptosis by inhibiting gamma-glutamyl cycle in TE1 cells. Phytother Res 2021;35:494-503.

45. Bai J, Kwok WC, Thiery JP. Traditional Chinese Medicine and regulatory roles on epithelial-mesenchymal transitions. Chin Med 2019;14:34.

46. Nourmohammadi S, Aung TN, Cui J, et al. Effect of Compound Kushen Injection, a Natural Compound Mixture, and Its Identified Chemical Components on Migration and Invasion of Colon, Brain, and Breast Cancer Cell Lines. Front Oncol 2019;9:314.

47. Jiang H, Ma P, Duan Z, et al. Ginsenoside Rh4 Suppresses Metastasis of Gastric Cancer via SIX1-Dependent TGF-β/Smad2/3 Signaling Pathway. Nutrients 2022;14:1564.

48. Wang X, He R, Geng L, et al. Ginsenoside Rg3 Alleviates Cisplatin Resistance of Gastric Cancer Cells Through Inhibiting SOX2 and the PI3K/Akt/mTOR Signaling Axis by Up-Regulating miR-429. Front Genet 2022;13:823182.

49. Kim MJ, Lee TH, Kim SH, et al. Triptolide inactivates Akt and induces caspase-dependent death in cervical

cancer cells via the mitochondrial pathway. Int J Oncol 2010;37:1177-85.

50. Chen RH, Tian YJ. Enhanced anti-tumor efficacy of aspirin combined with triptolide in cervical cancer cells. Asian Pac J Cancer Prev 2013;14:3041-4.

51. Lan YL, Wang X, Lou JC, et al. Bufalin inhibits glioblastoma growth by promoting proteasomal degradation of the Na+/K+-ATPase α1 subunit. Biomed Pharmacother 2018;103:204-15.

52. Huang H, Zhang W. Bufalin induced apoptosis of bladder carcinoma cells through the inactivation of Na+K+-ATPase. Oncol Lett 2018;16:3826-32.

53. Hsiao YP, Yu CS, Yu CC, et al. Triggering apoptotic death of human malignant melanoma a375.s2 cells by bufalin: involvement of caspase cascade-dependent and independent mitochondrial signaling pathways. Evid Based Complement Alternat Med 2012;2012:591241.

54. Zhu Z, Sun H, Ma G, et al. Bufalin induces lung cancer cell apoptosis via the inhibition of PI3K/Akt pathway. Int J Mol Sci 2012;13:2025-35.

55. Qi F, Inagaki Y, Gao B, et al. Bufalin and cinobufagin induce apoptosis of human hepatocellular carcinoma cells via Fas- and mitochondria-mediated pathways. Cancer Sci 2011;102:951-8.

56. Xie CM, Chan WY, Yu S, et al. Bufalin induces autophagy-mediated cell death in human colon cancer cells through reactive oxygen species generation and JNK activation. Free Radic Biol Med 2011;51:1365-75.

57. Wu SH, Hsiao YT, Kuo CL, et al. Bufalin Inhibits NCI-H460 Human Lung Cancer Cell Metastasis In Vitro by Inhibiting MAPKs, MMPs, and NF-κB Pathways. Am J Chin Med 2015;43:1247-64.

58. Hong SH, Kim GY, Chang YC, et al. Bufalin prevents the migration and invasion of T24 bladder carcinoma cells through the inactivation of matrix metalloproteinases and modulation of tight junctions. Int J Oncol 2013;42:277-86.

59. Qiu YY, Hu Q, Tang QF, et al. MicroRNA-497 and bufalin act synergistically to inhibit colorectal cancer metastasis. Tumour Biol 2014;35:2599-606.

60. Gai JQ, Sheng X, Qin JM, et al. The effect and mechanism of bufalin on regulating hepatocellular carcinoma cell invasion and metastasis via Wnt/β-catenin signaling pathway. Int J Oncol 2016;48:338-48.

61. Wang Z, Han J, Cui Y, et al. miRNA-21 inhibition enhances RANTES and IP-10 release in MCF-7 via PIAS3 and STAT3 signalling and causes increased lymphocyte migration. Biochem Biophys Res Commun 2013;439:384-9.

62. Borghouts C, Tittmann H, Delis N, et al. The intracellular delivery of a recombinant peptide derived from the acidic domain of PIAS3 inhibits STAT3 transactivation and induces tumor cell death. Mol Cancer Res 2010;8:539-53.

63. Sun H, Li Y, Quan X, et al. PIAS3/SOCS1-STAT3 axis responses to oxidative stress in hepatocellular cancer cells. Am J Transl Res 2021;13:12395-409.

64. Saini U, Suarez AA, Naidu S, et al. STAT3/PIAS3 Levels Serve as "Early Signature" Genes in the Development of High-Grade Serous Carcinoma from the Fallopian Tube. Cancer Res 2018;78:1739-50.

65. Rödel B, Tavassoli K, Karsunky H, et al. The zinc finger protein Gfi-1 can enhance STAT3 signaling by interacting with the STAT3 inhibitor PIAS3. EMBO J 2000;19:5845-55.

66. Brantley EC, Nabors LB, Gillespie GY, et al. Loss of protein inhibitors of activated STAT-3 expression in glioblastoma multiforme tumors: implications for STAT-3 activation and gene expression. Clin Cancer Res 2008;14:4694-704.

(English Language Editor: L. Huleatt)